

Association of limited valence patchy particles in two dimensions

John Russo,^a Piero Tartaglia^b and Francesco Sciortino^{*b}

Received 11th March 2010, Accepted 13th May 2010

DOI: 10.1039/c0sm00091d

We report simulations of a simple model of particles with limited valence in two dimensions and compare the numerical results with recent predictions based on the application of the Wertheim theory. The predictions for the fraction of formed bonds are rather accurate, except at low densities and temperatures, where enhanced bonding is found. Such differences are traced-back to the break-down of the approximation of absence of intra-cluster bonding. The enhanced bonding is thus attributed to the growing entropic cost of merging different clusters when the density is low, compared to the free-energy gain of forming an intra-cluster bond. The presence of closed bond loops in finite size clusters affects the location of the percolation locus, which is located at temperature lower than expected on the basis of the Flory–Stockmayer theory. Similarly, the critical region is shifted to temperatures smaller than the ones accessible with present time numerical resources, despite the implementation of efficient cluster moves. Only a weak evidence of a low-T gas–liquid phase separation between a very dilute gas phase and a low-density percolating liquid phase is found.

I. Introduction

Self-assembly of colloidal particles in two dimensions^{1–6} is receiving considerable interest, facilitated by the possibility of confining particles at interfaces⁷ or, playing with the different density of the particles as compared to the solvent, at the bottom of the sample holder.⁸ The study of two-dimensional self-assembly is facilitated by the possibility of imaging the surface on which particles aggregate, providing accurate time resolved information on the growth process and on the structure (equilibrium or arrested) of the system. Both amorphous and ordered structures have been observed, experimentally and/or *via* theoretical investigations.

While most previous work focused on aggregation properties of spherically interacting colloids (or mixtures of them), several efforts are now concentrating on the synthesis and self-assembly properties of patchy particles,⁹ in which patchiness results either from an anisotropic interaction potential (*e.g.* dipolar^{10–14} or quadrupolar¹⁵) or from different chemical composition of selected areas on the particle surface.^{16,17} The hope is to be able to build complex structures with a bottom up process, encoding the desired properties of the resulting material in the chemical-physical properties of the particles. Providing valence to colloids^{18–21} may result in a reconstruction of the molecular world on the nano and micro scale, as well as in the formation of new materials with novel and still unexplored possibilities.

In recent years, we have started a systematic theoretical and numerical study of the role of valence on the phase diagram and on the equilibrium and non-equilibrium dynamic properties of three-dimensional systems.^{19,22–27} We have shown that arrested states at low density—not mediated by a precursory phase

separation process²⁸—are possible if the valence of the interacting particles is limited to small numbers.^{29,30} In other words, particles able to form only a limited number of attractive contacts with their neighbors are characterized by a gas–liquid instability which becomes more and more suppressed (in temperature T and density ρ) on decreasing valence. This opens a large window of densities where the system forms a network structure in which the bond-lifetime becomes the leading element in controlling the dynamics. The possibility of forming equilibrium gels is intimately connected to the small valence. Support to this picture results from theoretical studies based on the Wertheim theory^{31–33} compared to accurate numerical investigations. Connections with the atomic and molecular network forming systems have also been provided.³⁴

In this article we numerically investigate, implementing the “virtual-move” Monte Carlo algorithm,³⁵ the aggregation properties of small valence particles in two dimensions (2d), with the aim of comparing with recently published 2d theoretical predictions.⁴ With respect to the three-dimensional case, despite the small valence, a significant fraction of particles participate in close loops of bonds, invalidating one of the basic assumptions of the first order thermodynamic perturbation theory of Wertheim. This results in an underestimation of the extent of bonding, which reveals essentially at low T and densities. As a consequence, the percolation line is not accurately predicted by the Flory–Stockmayer (FS) theory (as it was the case in three dimensions) and the gas–liquid phase separation is significantly suppressed compared to the Wertheim predictions.

II. The model

We focus on a system of particles modeled as hard-disks of diameter σ , whose circular contour is decorated by f bonding sites at fixed locations. Sites on different particles interact *via* a square-well potential. The interaction $V(\mathbf{1}, \mathbf{2})$ between particles **1** and **2** is

^aDipartimento di Fisica, Università di Roma La Sapienza, Piazzale A. Moro 2, 00185 Roma, Italy

^bDipartimento di Fisica and CNR-ISC, Università di Roma La Sapienza, Piazzale A. Moro 2, 00185 Roma, Italy. E-mail: francesco.sciortino@uniroma1.it

$$V(\mathbf{1}, \mathbf{2}) = V_{HD}(\mathbf{r}_{12}) + \sum_{i=1}^f \sum_{j=1}^f V_{SW}(\mathbf{r}_{12}^{ij}) \quad (1)$$

where the individual sites are denoted by i and j , V_{HD} is the hard-disk potential, $V_{SW}(x)$ is a square-well interaction (of depth $-u_0$ for $x \leq \delta$, 0 otherwise) and \mathbf{r}_{12} and \mathbf{r}_{12}^{ij} are respectively the vectors joining the particle-particle and the site-site (on different particles) centers. The parameter δ has the value $\delta = \frac{\sqrt{5 - 2\sqrt{3}} - 1}{2} \approx 0.119$, the largest value which guarantees that each site is engaged at most in one bond. Hence, with this choice of δ , each particle can form only up to f bonds. We note that in this model bonding is properly defined: two particles are bonded when their pair interaction energy is $-u_0$. Distances are measured in units of σ . Temperature is measured in units of u_0/k_B .

We study this model for an average valence $f = 2.1$, by simulating *via* MC a system composed of $N_2 = 4500$ bi-functional particles (with sites located at the poles) and $N_3 = 500$ three-functional ones (with sites symmetrically located on the equator). With this choice of the average valence the Wertheim prediction for the critical point lies in a temperature and density region accessible to simulations. Note also that mole fractions of three-coordinate particles of around 5% are typical in thin films of dipolar fluids.

We implement the so-called “virtual move” Monte Carlo (VMC) scheme,³⁵ which facilitates collective motion of clusters, allowing for faster equilibration times over standard single particle Monte Carlo moves. The algorithm starts by selecting a seed particle and proposing a virtual move to it (displacement or rotation). It then recruits all neighbours for which the virtual move of the seed particle is energetically disadvantageous. Every time a particle is added to the cluster, it adopts the virtual move and the recruitment algorithm is recursively extended to its neighbours. Once the cluster is identified, the virtual move is applied to all of its particles, and accepted with a rate that ensures detailed balance.

III Results

A. Bond probability

The key element in the Wertheim theory is the bond probability, *i.e.* the (normalized) number of bonds N_{bonds} present in the system, as a function of T and ρ . The normalization is performed by counting the maximum number of bonds N_{max} which can be formed in principle, equal to $N_{max} = \frac{2N_2 + 3N_3}{2}$. In this model, where the attractive interaction is of a square-well type, the number of bonds is directly proportional to the system potential energy, $E_{pot} = -u_0 N_{bonds} = -u_0 p_b N_{max}$, where p_b is the bond probability.

Fig. 1 shows the T -dependence of p_b for all investigated densities for both numerical and theoretical results (from ref. 4). Theoretical curves are based on the expression

$$\frac{p_b}{(1 - p_b)^2} = f\rho\Delta \quad (2)$$

where at low surface fraction η , the η dependence of Δ is given by⁴ $\Delta = 0.00437200 + 0.00642199 \eta + 0.00810584 \eta^2$. Such

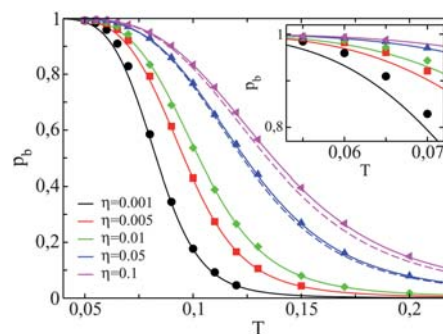


Fig. 1 The bond probability as a function of T for various occupied surface fractions η . Lines are evaluated with the Wertheim theory and the symbols refer to numerical simulations of a system with 4500 particles of functionality 2 and 500 particles of functionality 3, corresponding to $f = 2.1$. The dashed lines refer to the approximation $\Delta = 0.004372$ (corresponding to assuming for the radial distribution function of the hard-disks its ideal gas limit $g_{HD}(r) = 1$). The inset highlights the low T region, where deviations between the theoretical curves and the simulation results appear.

η dependence arises from the density dependence of the structure of the reference system (hard disk).

The bond probability continuously varies between zero, at large T , to a fully bonded state ($p_b = 1$), at low T . This suggests that the system essentially reaches its disordered ground state at a finite T , in equilibrium conditions. With “ground state” we indicate any fully bonded network, *i.e.* any lowest-energy configuration. The ground state is represented by highly degenerate network states (since there are many ways the network can assemble) and it is characterized by a high configurational entropy. The possibility to reach the ground state arises by the concomitant effect of the suppression of the phase separation induced by the small valence and by the absence of packing phenomena.^{30,23} The ability to reach a state very close to the disordered ground state at a finite T and in equilibrium condition (for example, in the simulation at $T = 0.055$ and $\eta = 0.1$, we observe the formation of more than 99.5 per cent of the bonds and their breaking and reforming processes) has important consequences for the formation of arrested states at low densities. Any further cooling does not alter the structure of the system and has the only effect of increasing the lifetime of the bonds (which can become permanent on the time scale of the experiment or of the simulation). No structural or bonding rearrangements (*i.e.* no aging) is expected, since the final ground state configuration has essentially been reached. This feature is similar to the one observed in chalcogenide glasses in the so-called reversibility window.³⁶

Comparing the theoretical predictions with the numerical results, we note that for $T > 0.07$ the parameter-free Wertheim theoretical predictions perfectly describe the simulation data. We note that the approximation $\Delta = 0.004372$ is indistinguishable from the density dependent solution up to $\eta = 0.05$, and even at $\eta = 0.1$ the effect of hard-disk structure is negligible. For lower T , when the system approaches a state in which all bonds are formed, deviations between numerical and theoretical results start to appear, and become more and more relevant on decreasing η . Interestingly, these deviations are in the direction

of increasing the number of bonds as compared to the theoretical predictions of Wertheim. Since these deviations are more evident at low packing, these cannot be attributed to an approximated evaluation of the neighbors in the reference system (since, at these low densities, the hard-disk radial distribution function which enters in the expression for Δ is essentially exact). Hence, the other main assumption of the theory, *i.e.* the absence of bond loops in the clusters, must break at low temperatures.

B. Structure in real space

To provide a direct evidence of a non negligible presence of bond loops in the system, we show in Fig. 2 the evolution of the 2d structure and the progressive clustering which takes place on increasing η and/or decreasing T . The system progressively forms larger and larger clusters which eventually span the entire simulated surface. Interestingly enough, larger clusters show an extensive intra-cluster bonding, a phenomenon which is not accounted for neither in the Wertheim³² nor in the Flory–Stockmayer³⁷ theories. Such intra-cluster bonding is not present when the same model is investigated in three dimensions,^{22,24} pointing to a different role of the entropy of closing a loop in different dimensions. This is in close analogy with quasi-two-dimensional dipolar fluids³⁸ where ring formation is clearly observed, as opposed to the analog 3D systems. At the lowest investigated T , where $p_b \approx 1$, only for $\eta \geq 0.05$ the largest cluster percolates, *i.e.* spans the simulation box.

C. Cluster structure

The structure of the clusters can be quantified by means of their fractal dimension.³⁹ To this aim, we evaluate the radius of

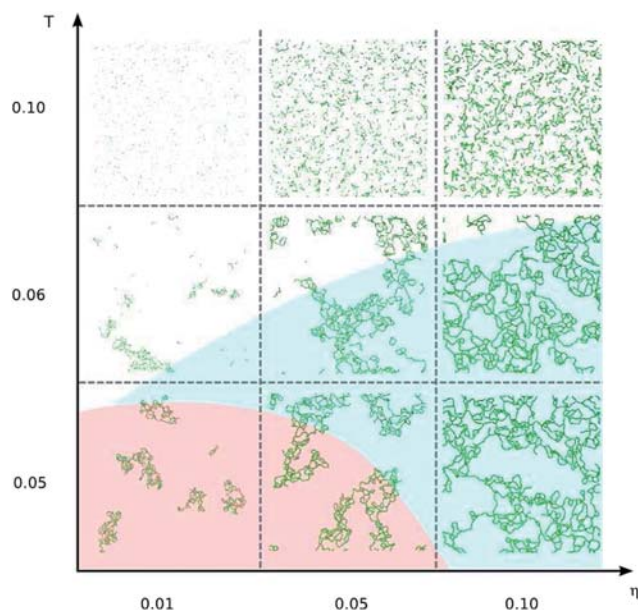


Fig. 2 Snapshots of an equilibrium typical configuration for a 5000 particles system at three different temperatures $k_B T / u_0 = 0.1, 0.06, 0.05$ and three different surface fractions $\eta = 0.01, 0.05, 0.1$. The two shaded area (dark and light) offer a pictorial indication of the percolating and phase separated configurations respectively (for the more precise numerical phase diagram see Fig. 10).

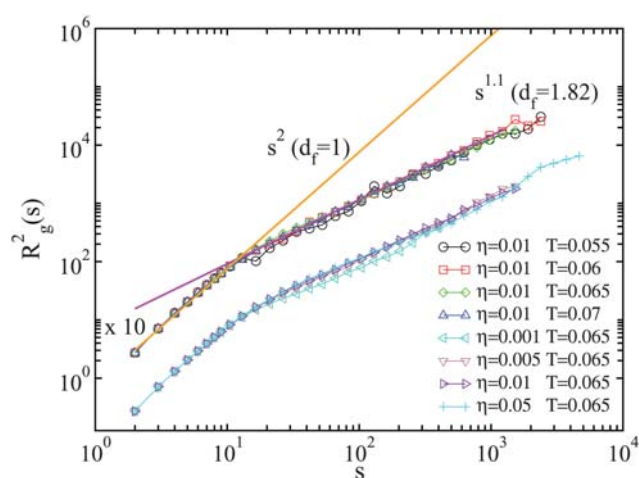


Fig. 3 Gyration radius of the aggregates as a function of their size. The data for $\eta = 0.01$ has been multiplied by a factor of 10 to avoid overlap with other sets and improve readability. Two distinct regimes are apparent: for $s \lesssim 10$ the gyration radius has a slope corresponding to $d_f = 1$ (*i.e.* linear chains) while for larger clusters ($s \gtrsim 10$) the fractal dimension is $d_f = 1.82$.

gyration $R_g^2(s)$ of a cluster composed by s particles, averaged over all clusters with the same size, defined as

$$R_g^2(s) = \left\langle \frac{1}{2s^2} \sum_{i,j,i \neq j} |\mathbf{r}_i - \mathbf{r}_j|^2 \right\rangle_s \quad (3)$$

For clusters of fractal dimension d_f , $\langle R_g^2(s) \rangle \sim s^{2/d_f}$. Fig. 3 shows this quantity along a constant η path and along a constant T path. For clusters of size less than 10, $d_f \approx 1$, consistent with a linear chain structure of small clusters (or, equivalently, consistent with the small amount of three-functional particles in the system). For larger clusters, branching becomes relevant and the fractal dimension increases toward two. The best fit exponent suggest that $d_f \approx 1.8$ on increasing p_b (close to the percolation universality class value⁴⁰ of $d_f = 91/48$). The fractal dimension d_f is close to the embedding space dimension $d = 2$ which, thanks to the large fraction of loops, makes the clusters very compact as compared to ideal (*i.e.* loop-less) branched polymers.

The structure of the cluster is found to be slightly dependent on p_b , as can be noticed comparing the data at constant T around cluster sizes of the order 100. A systematic effect is observed in the direction of smaller $R_g(s)$ values (*i.e.* more compact clusters) for smaller η , and hence smaller p_b . This is due to the fact that the structure of the cluster depends on the relative fraction of bi- and three-functional particles. For smaller p_b values, large clusters contain a larger fraction of three-functional particles as compared to the bulk concentration. At fixed cluster size s , on increasing p_b , the relative concentration of bi-functional particles increases and $R_g(s)$ grows.

D. Structure in wave-vector space

The structure of the system can be quantified by evaluating the structure factor $S(q)$. In associating systems, $S(q)$ increases significantly at small wavevectors q , due to the coherent scattering signal of the particles aggregated into clusters. In the case

of highly polydisperse systems, in the limit of small concentrations (*i.e.* in the limit of an ideal gas of clusters of different size, as in the present case) the behavior of $S(q)$ at very small q (such that the inverse scattering vector is significantly larger than the largest cluster size) satisfies the Guinier law.⁴¹ Since the system is polydisperse, summing over all cluster sizes, one recovers

$$S(q) = \frac{\sum_s n_s s^2 \left(1 - \frac{q^2 R_g(s)^2}{2}\right)}{\sum_s s n_s} \quad (4)$$

Here the scattering for $q \rightarrow 0$, $S(0) = \frac{\langle s^2 \rangle}{\langle s \rangle}$, depends only on the second moment of the cluster size distribution n_s . For q^{-1} of the order of the typical cluster size one expects $S(q) \sim q^{-d_f}$ instead. Fig. 4 shows the calculated two-dimensional structure factor along two different isochores. At small η , the ideal gas approximation is rather well satisfied, as can be seen from the comparison with the expected low q theoretical expression. At larger q [inset of Fig. 4(a)] it is possible to clearly detect the two regions of fractal scaling, one associated to the branched clusters and one associated to the chain region. At larger η , the excluded volume interaction between the cluster does not allow us to observe the Guinier law. The small q regime reflects now the cluster–cluster interaction more than the form factor. It is interesting to observe that $S(q)$ increases with cooling but then it saturates to a constant T independent behavior. The saturation of $S(q)$ reflects the fact that the structure of the system does not change any longer with T , due to the fact that $p_b \rightarrow 1$ and all particles are connected in one large spanning cluster. The system

has reached an almost fully bonded (disordered ground state) configuration and further cooling does not modify the structure. This fully bonded equilibrium state is what has been referred to as an equilibrium gel.²⁹

We note on passing that accurate $S(q)$ data require the equilibration of the diffusional processes on distances of the order of q^{-1} . For small q , this requires waiting for clusters diffusing over distances comparable to the size of the simulation box, which in two dimensions and for small densities may become a prohibitively long time. Indeed, if one follows the evolution of $S(q)$ in time with a standard MC algorithm, one observes that a peak, similar to the one observed in spinodal decomposition, develops and grows. Then, the signal at small q progressively grows generating the correct equilibrium Guinier law for very long times. The virtual move algorithm, by displacing clusters of particles over longer distances, facilitates the formation of the equilibrium density fluctuations at small q . While the finite q peaks are not an equilibrium property, they may have a significance in kinetic studies when the system is quenched to rather low temperature so that the system behaves similarly to an irreversibly aggregating system.^{42–44} It is interesting to observe that these transient peaks are observed also in regions where, at long time, the system is in the stable fluid phase.

E. Loops

According to the Flory–Stockmayer theory, bond loops are only contained in the infinite spanning cluster, and can be calculated as the difference between the number of bonds and the number of particles in the spanning cluster:

$$N_\infty^{\text{loops}} = N_\infty^{\text{bonds}} - NP_\infty + 1 \quad (5)$$

where the subscript ∞ refers to quantities in the spanning cluster, and P_∞ is the fraction of particles belonging to the infinite cluster. In the Flory postgel assumption, the terms in eqn (5) can be calculated from the knowledge of the number density of *finite* size clusters containing n three-functional particles and l bifunctional ones

$$\rho_{nl} = \rho_3 \frac{(1-p_b)^2}{p_3 p_b} [p_3 p_b (1-p_b)]^n [(1-p_3) p_b]^l w_{nl} \quad (6)$$

$$w_{nl} = 3 \frac{(l+3n-n)!}{l! n! (n+2)!}$$

where w_{nl} is a combinatorial contribution,³⁷ ρ_3 is the number density of three-functionalized particles and $p_3 = 3N_3/(2N_2 + 3N_3) = 0.1428$ is the probability that a randomly chosen binding site belongs to a three-functional particle. We then have

$$N_\infty^{\text{bonds}} = N^{\text{bonds}} - \sum_{l,n,l+n>0} (l+n-1) S \rho_{nl}$$

$$NP_\infty = N - \sum_{l,n,l+n>0} (l+n) S \rho_{nl}$$

where S is the total surface. In Fig. 5 we show the average number of bond loops per particle for all the simulated state points (symbols), together with the prediction of eqn (5) (full line). The results show that a non-negligible number of loops

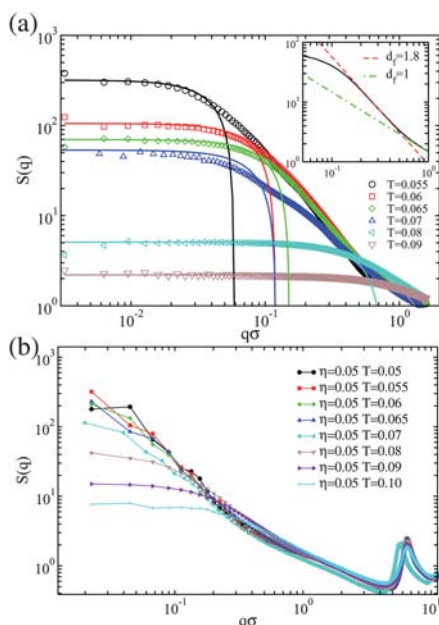


Fig. 4 Structure factor for different T at $\eta = 0.001$ (a) and $\eta = 0.05$ (b).

The full line in (a) is $S(q) = \frac{\langle s^2 \rangle}{\langle s \rangle} \left(1 - \frac{q^2 R_g^2}{2}\right)$, with the appropriate mean cluster size and average gyration radius. The inset shows that the region $0.1 < q\sigma < 1$ can be well represented with the law $S(q) \sim q^{-d_f}$ with $d_f = 1.8$, while $d_f = 1$ for larger q . Note that in (b), no changes in the structure factor are visible at low T , a signature that most of the bonds have been formed and no further structural changes take place on further cooling.

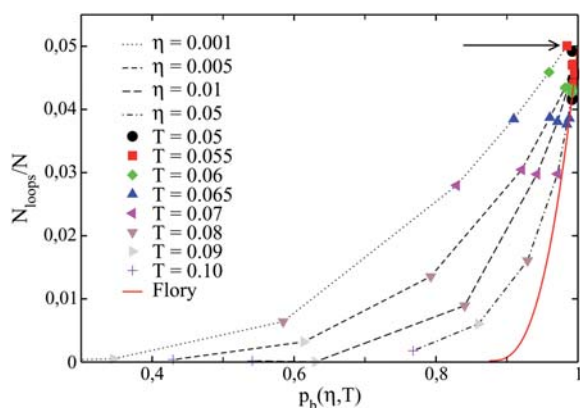


Fig. 5 Average number of loops per particle. The same symbol is used for simulations at equal temperature, while dashed lines connect simulations at equal density. The full line is the Flory-Stockmayer prediction for the number of loops in the percolating cluster (for $p_b > p_c = 0.875$) and the arrow marks the predicted number of loops per particle in the ground state ($p_b = 1$). The results clearly show that the number of loops always exceeds the FS prediction, and that more loops are formed as the density is lowered.

forms in finite size clusters, and that more loops are formed as η is lowered, suggesting that intra-cluster bonding is indeed promoted by the low density. This is consistent with the consideration that the entropic cost of merging two distinct clusters by forming a bond increases on decreasing η .

We also evaluate the distribution of primitive rings in the network, employing the definition and algorithm reported in ref. 45. By this definition, a primitive ring is a ring that cannot be decomposed into two smaller rings, that is, given any two particles of the primitive ring, the shortest path between the two particles is on that ring. Fig. 6 shows the number of rings observed in the simulations at $T = 0.07$ as a function of η . We note that the most abundant rings are composed of about 10 particles. Within the numerical error, the large ring-size tail of the distribution appears to converge at large η to a density invariant distribution which can be described by an exponential tail with a characteristic ring length of about 14 particles.

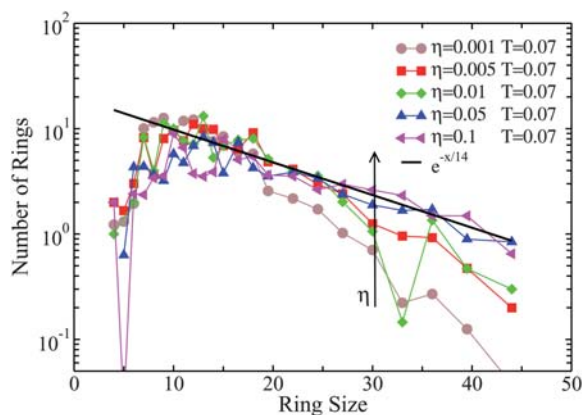


Fig. 6 Distribution of bond loops (rings) at $T = 0.07$ for different densities. As the density increases the distribution can be described by an exponential tail with a characteristic ring length of about 14 particles.

To better quantify the connectivity of the system we calculate the cluster size distribution ρ_s (expressed as number density of clusters of size s , so that $\sum_s s \rho_s = \rho$), defined as

$$\rho_s = \sum_{ln, l+n > 0} \rho_{nl} \delta_{s, n+1} \quad (7)$$

where ρ_{nl} are the cluster densities given by eqn (6).

In the analysis of the configurations, particles are considered to be members of the same cluster if there is a sequence of bonds joining them. The results are reported in Fig. 7, together with the Flory-Stockmayer (FS) predictions (at the same bond probability).³⁷

Consistent with the ring statistic results, only at high T (where rings are missing) the FS predictions agree with the numerical results. The agreement between FS predictions and simulations also improves at higher η (results not shown). When the system starts to form clusters with size larger than 10–20, the number of large size clusters observed significantly overshoots the FS predictions.

Close to percolation (see Fig. 8), data follow a power-law with an apparent exponent $\tau \approx 1.66 \pm 0.05$. This value differs from

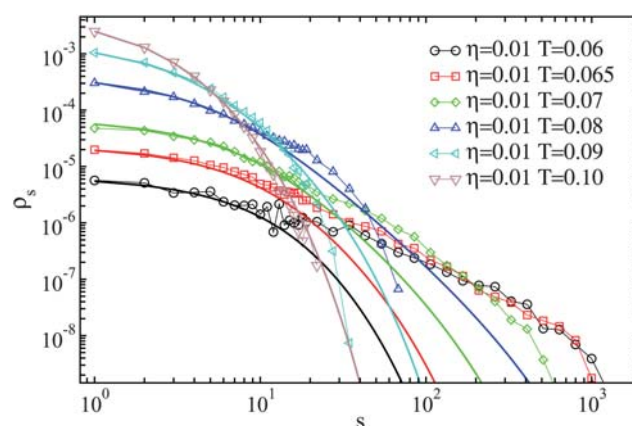


Fig. 7 Cluster size distribution for $\eta = 0.01$ at several T . Full lines are predictions of the FS theory evaluated according to eqn (7) with the same p_b .

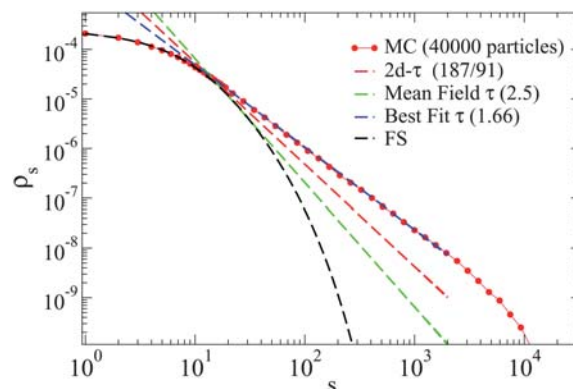


Fig. 8 Cluster size distribution close to percolation ($T = 0.078$, $\rho = 0.1$). To minimize size effects, 40 000 particles have been simulated. The different straight lines show the theoretical predictions for mean-field and 2d-percolation, as well as the best fitting slope of the numerical n_s . The cluster size predicted by the Flory-Stockmayer theory is also reported, but its range of validity is limited to only small clusters.

the expected two dimensional site or bond percolation prediction $\tau = 187/91$,⁴⁶ suggesting that we are not sufficiently close to percolation to detect the asymptotic exponent. We note that in the corresponding 3d case,²² even rather close to percolation the cluster size distribution was properly predicted by the mean field scaling exponent $\tau = 2.5$. This difference again stresses the relevant role of the bond loops in two dimensions.

Within the FS approach it is possible to evaluate, at any fixed p_b value, the length distribution $\rho_2(s)$ of chains formed only by two-functional particles. This distribution, normalized in such a way that $\sum s\rho_2(s) = N_2/S$, is

$$\rho_2(s) = \rho_2(1 - p_2 p_b)^2 (p_2 p_b)^{s-1} \quad (8)$$

where $p_2 = 2N_2/(2N_2 + 3N_3) = 0.8571$ is the probability that a randomly chosen binding site belongs to a bifunctional particle. The $\rho_2(s)$ distribution is thus always exponential. At low T , when $p_b \rightarrow 1$, the distribution becomes controlled only by the relative fraction of two-functional particles. Indeed, when $p_b \rightarrow 1$, the average distance \bar{l} between branching points in the network becomes only a function of p_2 , *i.e.* $\bar{l} = 1/(1 - p_2)$. Fig. 9 compares the FS predictions with the numerical results. The bond probability in the theoretical expression is the one predicted by

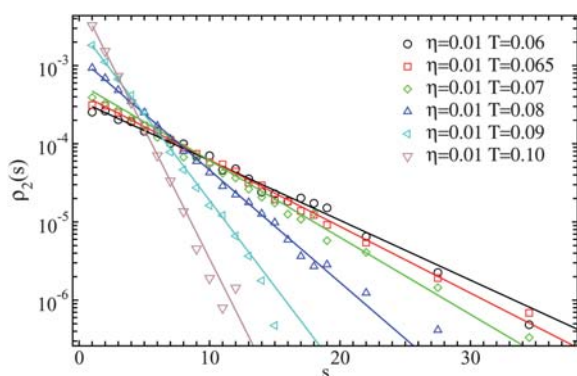


Fig. 9 Cluster size distribution for chains of bifunctional particles at $\eta = 0.01$. Dashed lines are parameter free theoretical predictions based on eqn (8) with p_b from eqn (2).

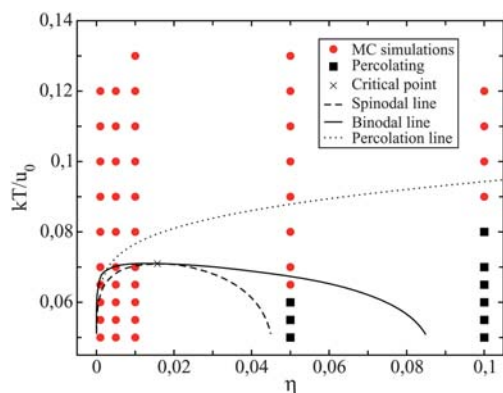


Fig. 10 Phase diagram for the case of the functionality $f = 2.1$. Lines are theoretical predictions based on the Wertheim theory (from ref. 4), and the cross symbol (\times) is the predicted critical point. Symbols are numerical results for percolating and non percolating state points.

Wertheim (eqn (2)). The distribution $\rho_2(s)$, which does not involve loops by construction, is perfectly described by eqn (8).

A global view of the connectivity properties of the system is reported in Fig. 10, where state points which have been found to be characterized by spanning clusters are indicated. We also show the predicted FS line of percolation. As expected, percolation is found at temperatures well below the FS prediction, since a large fraction of bonds is “wasted” in intra-cluster connections which do not favor the formation of a spanning cluster. The same figure reports also the Wertheim prediction for the spinodal and the gas-liquid coexistence for the present model. It is interesting to note that the presence of intra-cluster bonds, by depressing the percolation line, has also a profound impact on the gas-liquid phase separation. Indeed, if the formation of bonds can be realized without connecting different clusters, then the driving force for phase separation (*i.e.* for creating an infinite size cluster⁴⁷) decreases. Moreover, percolation *via* physical bonds is a pre-requisite for phase-separating, as shown in the 80s by Coniglio and coworkers.⁴⁸ In the case of the simple short-range square-well potential, this means that the gas-liquid critical point (which is characterized by diverging correlation lengths) must be located in the percolating part of the (T, η) plane.

The natural question which arises is if the intra-cluster bonding shifts the critical point to smaller T than expected on the basis of the Wertheim theory or if it completely suppresses the critical point. This last possibility would be the case if the intra-clustering bonding generates fully bonded structures, which are then inert for what concern the phase separation process, in analogy to the micelle formation process in surfactants.^{49–51} However, in the present 2d system, a visual inspection of the low temperature ($T = 0.05$) configurations [(d) and (e) in Fig. 2] reveals that: (i) for $\eta \leq 0.05$ the observed cluster structure is always composed by very few clusters; (ii) several reactive (unbonded) sites remain located on the cluster perimeter; (iii) the final configurations span the simulation box only when $\eta \geq 0.05$, suggesting that the density of the liquid branch spinodal should have approximately this value. These data suggest that, in order to achieve almost full bonding at small η (as expected on the basis of the p_b data reported in Fig. 1), the system is forced to phase separate.

IV. Conclusions

In this article we have examined the equilibrium properties of a mixture of bifunctional and three-functional patchy particles in two dimensions. The study of this model is very relevant for the field of low-valence colloidal suspensions whose motion is constrained in 2d. Both equilibrium and nonequilibrium properties of the three dimensional version of this model have been extensively studied,^{24,52} so that a direct comparison with the present results makes it possible to uncover the effects of the confinement to a surface.

The short-range and limited-valence nature of the interactions, together with the low densities considered in the present work, determine very long equilibration times inaccessible with conventional methods. To overcome this difficulty we have adopted the “virtual move” Monte Carlo algorithm, successfully covering a large region of the $\eta - T$ phase diagram. The

numerical results have then been compared with the theoretical predictions of the Wertheim theory, which is known to give very accurate estimates for the corresponding three-dimensional systems.²²

First, we have considered the η and T dependence of the bond probability (p_b), showing that it is possible to reach the ground state at finite T . The Wertheim theory predictions for p_b prove very accurate for $T > 0.07$, but clearly underestimate the real number of bonds at lower temperatures, and more so at lower values of η . The failing of the Wertheim theory at low η and T is attributed to the large number of loops in finite size clusters, which the theory does not take into account. The significant presence of loops is peculiar to the 2d system, being very different from the previously studied three-dimensional case.^{22,24} These differences can be traced down to the lower entropic cost of forming a loop in two dimensions rather than in three, making the formation of intra-cluster bonds more convenient in the former case.

We have then characterized the clusters structure by means of their fractal dimension. The radius of gyration of the clusters shows two distinct behaviours: up to ten particles, the fractal dimension is $d_f \approx 1$, therefore indicating a linear chain structure of the smaller clusters; for larger clusters, we obtain a fractal dimension of $d_f \approx 1.8$. We also note that the structure of the clusters has a small dependence on the bond probability. Focusing at clusters of the same size, the ones at lower η (*i.e.* lower p_b) are richer in three-functional particles and consequently their radius of gyration is smaller (since there is more branching).

Further structural information on our system is obtained by studying the structure factor properties at low- q . This is a difficult task at very low η , because it is necessary to fully equilibrate the diffusional processes over distances of the order of q^{-1} . The VMMC algorithm employed in this study has proven essential in order to obtain a full equilibration of the system and avoid spurious artifacts. The increase of the structure factor at small q -vectors satisfies the Guinier law, showing that, at least for the low η , the system can be viewed as a collection of independent and polydispersed clusters. The value at zero wave-vector is predicted from the second moment of the cluster size distribution, and the low- q decay gives us the correct fractal dimension.

We have also quantified the number of loops in the $T = 0.07$ systems at different η , showing that the distribution of ring-sizes has a peak at about ten particles and, at high volume fractions, displays an exponential tail with a characteristic length of 14. The Flory–Stockmayer predictions for the cluster-size distribution, for sizes larger than 10–20, fail due to the abundant number of loops in large clusters. It is an open question why, even close to percolation, the observed τ significantly differs from the expected 2d random percolation universality class.

Bond loops have also a strong influence on the phase diagram. With respect to the Wertheim predictions, we note a strong suppression of the percolation line and the critical region, to low temperatures and η . In the T -window which we have been able to explore, only at the lowest studied $T = 0.05$ we have observed the formation, for $\eta \approx 0.05$, of almost fully bonded clusters which barely percolate. This is suggestive of the presence of phase separation at lower η . Studies at higher average valence (where the critical point would be located at larger temperatures) can

help clarifying this issue. Finally, results reported in this manuscript provide an accurate set of data to compare with predictions of future theoretical approaches in which the role of loop formation can be explicitly taken into account.

Acknowledgements

We acknowledge support from NoE SoftComp NMP3-CT-2004-502235, ERC-226207-PATCHYCOLLOIDS and ITN-234810-COMPLOIDS. We thank C. De Michele, E. Bianchi and F. Romano for comments.

References

- 1 F. Ebert, G. Maret and P. Keim, *Eur. Phys. J. E*, 2009, **29**, 311.
- 2 N. Hoffmann, F. Ebert, C. N. Likos, H. Löwen and G. Maret, *Phys. Rev. Lett.*, 2006, **97**, 078301.
- 3 N. Hoffmann, C. Likos and H. Löwen, *Mol. Phys.*, 2007, **105**, 1849.
- 4 P. Tartaglia and F. Sciortino, *J. Phys.: Condens. Matter*, 2010, **22**, 104108.
- 5 N. Geerts and E. Eiser, *Soft Matter*, 2010, **6**, 664.
- 6 A. G. Vanakaras, *Langmuir*, 2006, **22**, 88.
- 7 E. M. Herzig, K. A. White, A. B. Schofield, W. C. K. Poon and P. S. Clegg, *Nat. Mater.*, 2007, **6**, 966.
- 8 L. Hong, A. Cacciuto, E. Luijten and S. Granick, *Langmuir*, 2008, **24**, 621.
- 9 T. M. Hermans, M. A. C. Broeren, N. Gomopoulos, P. van der Schoot, M. H. P. van Genderen, N. A. J. M. Sommerdijk, G. Fytas and E. W. Meijer, *Nat. Nanotechnol.*, 2009, **4**, 721.
- 10 R. Blaak, M. A. Miller and J.-P. Hansen, *Europhys. Lett.*, 2007, **78**, 26002.
- 11 K. V. Workum and J. F. Douglas, *Phys. Rev. E: Stat., Nonlinear, Soft Matter Phys.*, 2005, **71**, 031502.
- 12 G. T. Gao, X. C. Zeng and W. Wang, *J. Chem. Phys.*, 1997, **106**, 3311.
- 13 P. I. C. Teixeira, J. M. Tavares and M. M. Telo da Gama, *J. Phys.: Condens. Matter*, 2000, **12**, R411.
- 14 J. Fornleitner, F. Lo Verso, G. Kahl and C. N. Likos, *Soft Matter*, 2008, **4**, 480.
- 15 M. Dijkstra, J. Hansen and P. A. Madden, *Phys. Rev. E: Stat. Phys., Plasmas, Fluids, Relat. Interdiscip. Top.*, 1997, **55**, 3044.
- 16 A. Walther and H. Müller, *Soft Matter*, 2008, **4**, 663.
- 17 L. Hong, A. Cacciuto, E. Luijten and S. Granick, *Langmuir*, 2008, **24**, 621.
- 18 G. Zhang, D. Wang and H. Möhwald, *Angew. Chem., Int. Ed.*, 2005, **44**, 1.
- 19 C. De Michele, S. Gabrielli, P. Tartaglia and F. Sciortino, *J. Phys. Chem. B*, 2006, **110**, 8064.
- 20 D. J. Kraft, J. Groenewold and W. K. Kegel, *Soft Matter*, 2009, **5**, 3823.
- 21 F. W. Starr and F. Sciortino, *J. Phys.: Condens. Matter*, 2006, **18**, L347.
- 22 E. Bianchi, P. Tartaglia, E. La Nave and F. Sciortino, *J. Phys. Chem. B*, 2007, **111**, 11765.
- 23 E. Bianchi, P. Tartaglia, E. Zaccarelli and F. Sciortino, *J. Chem. Phys.*, 2008, **128**, 144504, 0802.2466.
- 24 J. Russo, P. Tartaglia and F. Sciortino, *J. Chem. Phys.*, 2009, **131**, 014504.
- 25 F. Sciortino, C. De Michele, S. Corezzi, J. Russo, E. Zaccarelli and P. Tartaglia, *Soft Matter*, 2009, **5**, 2571.
- 26 G. Foffi and F. Sciortino, *J. Phys. Chem. B*, 2007, **111**, 9702.
- 27 F. Romano, E. Sanz and F. Sciortino, *J. Phys. Chem. B*, 2009, **113**, 15133.
- 28 P. J. Lu, E. Zaccarelli, F. Ciulla, A. B. Schofield, F. Sciortino and D. A. Weitz, *Nature*, 2008, **453**, 499.
- 29 E. Zaccarelli, *J. Phys.: Condens. Matter*, 2007, **19**, 323101.
- 30 E. Bianchi, J. Largo, P. Tartaglia, E. Zaccarelli and F. Sciortino, *Phys. Rev. Lett.*, 2006, **97**, 168301.
- 31 M. Wertheim, *J. Stat. Phys.*, 1984, **35**(1–2), 19.
- 32 M. Wertheim, *J. Stat. Phys.*, 1986, **42**(3–4), 459.
- 33 D. Chandler and L. R. Pratt, *J. Chem. Phys.*, 1976, **65**, 2925.
- 34 F. Sciortino, *Eur. Phys. J. B*, 2008, **64**(3–4), 505.
- 35 S. Whitelam and P. L. Geissler, *J. Chem. Phys.*, 2007, **127**, 154101.

- 36 S. Chakravarty, D. G. Georgiev, P. Boolchand and M. Micoulaut, *J. Phys.: Condens. Matter*, 2005, **17**, L1.
- 37 P. J. Flory, *Principles of polymer chemistry*, Cornell University Press, Ithaca and London, 1953.
- 38 J. M. Tavares, J. J. Weis and M. M. Telo da Gama, *Phys. Rev. E: Stat., Nonlinear, Soft Matter Phys.*, 2002, **65**, 061201.
- 39 T. Vicsek, *Fractal Growth Phenomena*, World Scientific, Singapore, 1989.
- 40 M. Rubinstein and R. H. Colby, *Polymer Physics*, Oxford University Press Inc., New York, 2003.
- 41 B. J. Berne and R. Pecora, *Dynamic Light Scattering: With Applications to Chemistry, Biology, and Physics*, Dover Publications, 2000.
- 42 M. Carpineti and M. Giglio, *Phys. Rev. Lett.*, 1992, **68**, 3327.
- 43 F. Sciortino and P. Tartaglia, *Phys. Rev. Lett.*, 1995, **74**, 282.
- 44 F. Sciortino, A. Belloni and P. Tartaglia, *Phys. Rev. E: Stat. Phys., Plasmas, Fluids, Relat. Interdiscip. Top.*, 1995, **52**, 4068.
- 45 X. Yuao and A. N. Cormack, *Comput. Mater. Sci.*, 2002, **24**, 343.
- 46 D. Stauffer and A. Aharony, *Introduction to Percolation Theory*, Taylor and Francis, London, 1992, 2nd edn.
- 47 T. L. Hill, *An Introduction to Statistical Thermodynamics*, Dover Pubns, 1987.
- 48 A. Coniglio and W. Klein, *J. Phys. A: Math. Gen.*, 1980, **13**, 2775.
- 49 F. Sciortino, A. Giacometti and G. Pastore, *Phys. Rev. Lett.*, 2009, **103**, 237801.
- 50 A. Z. Panagiotopoulos, M. A. Floriano and S. K. Kumar, *Langmuir*, 2002, **18**, 2940.
- 51 D. W. Cheong and A. Z. Panagiotopoulos, *Langmuir*, 2006, **22**, 4076.
- 52 J. Russo and F. Sciortino, *Phys. Rev. Lett.*, 2010, **104**, 195701.